THREE-DIMENSIONAL ANALYSIS OF THE LATTICE CONFINEMENT EFFECT ON ION DYNAMICS IN CONDENSED MATTER AND LATTICE EFFECT ON THE D-D NUCLEAR REACTION CHANNEL

NUCLEAR RACTIONS IN SOLIDS

KEYWORDS: *deuterons nuclear interaction in palladium*

VITTORIO VIOLANTE,* and AMALIA TORRE
Associazione Euratom-ENEA sulla Fusione, Centro Ricerche Frascati
C.P. 65 - 00044 Frascati, Rome, Italy

GIOVANNA SELVAGGI and GEORGE H. MILEY
University of Illinois, Fusion Studies Laboratory, 205 Nuclear Engineering Laboratory
103 South Goodwin Avenue, Urbana, Illinois 61801

Received February 18, 2000
Accepted for Publication July 18, 2000

A three-dimensional analysis of the dynamics of hydrogen isotopes confined within a metal lattice, like palladium or nickel, is presented. It is assumed that the concentration of the hydrogen isotopes, as an atomic fraction, is close to unity and that coherent oscillations of the metal atom electrons near to the Fermi level take place. Coherent oscillations of the Fermi-level electrons in the metal lattice can produce an oscillating electric field within the cell and hence produce a radio-frequency oscillation of ions like protons or deuterons. The trajectories of the ions can be studied by means of the equations of motion. The results show that under proper initial conditions, the closest distance of approach between two ions or between an ion and the nucleus of an atom of the host metal lattice can be reduced below 0.1 Å. An evaluation of the excess of heat production has been done for the D-D reaction within a Pd lattice by approximating the reaction both to an s-wave and a d-wave process, respectively. Last, the effect of the lattice field, which causes the collisions between ions, on the nuclear reaction channel for the D-D reaction is investigated by evaluating the transition probability for a stimulated decay.

I. INTRODUCTION

The mounting evidence nuclear reactions can occur in solids has enhanced the scientific interest in this research field. After the astonishing results given 10 yr ago by Fleischmann and Pons,[1] the main difficulty encountered by the majority of the experimentalists has been the lack of reproducibility, which created skepticism in the scientific community. The work done during the last 10 yr has mainly been oriented to improving the reproducibility of the excess heat production, to make accurate measurements of nuclear emissions, and to study new nuclear processes in condensed matter. We have to highlight that, generally, this research activity has been carried out with particular attention both to correlate the phenomena with the state of the system and to study crucial aspects of material science associated with the loading (e.g., D-metal atom ratio) of the electrode.

Kunimatsu et al.[2] and McKubre et al.[3] demonstrated that the excess heat production is a threshold phenomenon depending on the loading ratio of D in Pd; McKubre found that the lack of equilibrium in the Pd-D system is another necessary condition to have excess heat production.[4] The effect of the metallurgical structure on the H isotopes equilibrium concentration in the metal has been

*E-mail: violante@frascati.enea.it

theoretically and experimentally investigated.[5–9] The stress field that depends on the microstructure of the metal modifies the chemical potential of the solute with a significant effect on the achievable loading.

Other experimentalists obtained a good reproducibility by using low-dimensionality samples, like thin films, thin wires, or powdered metal, where the effect of the stress field is reduced.[10–12]

A remarkable improvement has been recently obtained in the investigation of the nuclear ashes. Arata and Zhang,[12] Gozzi et al.,[13] and Miles and Bush[14] measured ^{4}He formed during excess heat production obtained by means of electrochemical loading of D in Pd. Botta et al.[15] measured ^{4}He during a gas-loading experiment of D in Pd.

Products of nuclear transmutations have been obtained by Miley et al.[10] during electrolysis of light water on single-layer and multilayer thin films of Ni and Pd on polymeric spherical supports. These products are ashes of proton-metal reactions and like ^{4}He production provide vital insight into the reaction mechanism and heat production in this unique situation where the metallic electrode is involved in the reaction. Since such products are actually easier to measure than ^{4}He in D-D systems, more is known about reaction products in this new field (termed low-energy nuclear reaction). Preparata[16] studied the probability of a nuclear reaction in a metal lattice on the basis of a coherent behavior of electron and deuteron plasmas in the lattice. Hora et al.[17] gave a possible explanation for the presence of nuclear reactions in condensed matter on the basis of the screening improvement by electrons at interfaces like grain surfaces or metal-to-metal interfaces (swimming electron theory). Hagelstein[18] and Swartz[19] proposed a coupling between the excited ^{4}He nucleus and the lattice phonon field as an energy transfer mechanism in the cold fusion process.

There are many other contributions to the open literature that confirm both the existing interest in this research field and the effort expended to have a better understanding of these new phenomena in condensed matter; see, for example, the proceedings of the international conferences on cold fusion.[2–7,11]

A two-dimensional (2-D) analysis of ion dynamics within a metal lattice cell has been proposed[20–22] by one of the authors (V.V.) to justify the strong reduction of the distance between particles in a lattice, taking advantage of an analogy between the ion traps and the lattice cell when coherent oscillations of the Fermi-level electrons take place. The lattice cell can be seen as a confinement space (i.e., trap). Plasmons[23–24] that are coherent oscillations of the Fermi-level electrons of a lattice (e.g., Ni, Pd) seem to play a key role in ion dynamics in condensed matter.

The lattice electrons that are weakly bound can participate in coherent oscillations when they are moved through a short distance relative to the fixed background of the positive charge of the lattice. Such a coherent behavior has been observed and widely investigated near the metal/gas, metal/electrolyte interfaces, in which case a region of several thousands of angstroms from the surface seems to be involved; it has also been shown that surface roughness or suitable values of the dielectric constant at the surface interface can enhance the phenomena.[25–28]

A 3-D analysis is presented in this paper, generalizing the model of Refs. 20, 21, and 22, where the particles are assumed to move on a plane, to investigate if the study in the 3-D space modifies the results obtained by collapsing the problem to a plane movement as has been done in the 2-D calculations. In this case, volumetric effects are studied.

The equations of motion in the lattice cell coordinate system are numerically solved to follow the track of a moving particle (deuteron or proton) with respect to a fixed target. The resulting trajectories of deuterons suggest the consideration of the possibility for a nuclear reaction in the lattice. Therefore, a preliminary evaluation is possible of the effect of the lattice electromagnetic field on the nuclear process, proposed in Sec. V of this paper, where electromagnetic coupling between the excited compound ^{4}He nucleus, formed by the D-D reaction and the electric field created by the coherent oscillations of the electrons are considered. This evaluation is carried out on the basis of the assumption that energy of the decaying ^{4}He nucleus is given back to the lattice (that behaves like an infinite reservoir not strongly affected by the nuclear decay, as will be explained in the following) and that the stimulated decay is not a radiative process. The mechanism for the energy transfer between the decaying nucleus and the lattice is outside the scope of this work. Mechanisms (depending on the assumed decay time) for energy transfer from the nucleus to the lattice have been proposed in the literature.[16,18,19]

The model for the ion dynamics is presented in Sec. II, while the results of the calculations with the particle trajectories are shown in Sec. III.

The effect of the lattice field on the nuclear process producing ^{4}He as ashes of the D-D reaction is treated in Sec. IV. Section V is concerned with the evolution of the excess heat production, taking into account the collision probability obtained from the dynamics analysis and the decay of the excited ^{4}He in the lattice.

II. MODELING PARTICLE DYNAMICS IN THE LATTICE

The model has been developed to account for the dynamics of two particles moving through a lattice cell. The particles can be protons or deuterons or one of these isotopes and a nucleus of a lattice metal atom. However, in the model, all the combinations of charges and masses are allowed for the two particles, which both can be initially moving; however, in the present context, we assume that one of them, the target, is initially at rest, e.g.,

in a tetrahedral site if it is a proton or a deuteron, or in some lattice position if the target is the nucleus of a metal atom.

In this model, the moving ion particle (the shot) is assumed to enter the lattice trap by diffusion, and hence with random position, direction, and energy (assumed in the thermal range). The shot entering the cell gains energy from the lattice electromagnetic field.

The calculations can be also carried out within a Monte Carlo loop to estimate the probability for a collision event (minimum distance between the particles on the order of 0.1 Å or less, i.e., shorter than the moving particle wavelength).

The target, even if initially at rest, begins to move when the energy of interaction gained from the shot becomes greater than its binding energy in the lattice (typically ≈ 1 eV).

Before going on with the mathematical description of the system, it is convenient to underline the basic assumptions of the model.

The H isotopes can be considered as ions in the lattice[29–31] (simply because of the higher electronegativity of the metal atoms). Within the framework of a 3-D picture, the region between two parallel planes of the lattice cell can be visualized as an electromagnetic field region that can trap the ions for a proper frequency; then the effect of the electrodynamic containment on their dynamics can be studied by means of the equations of motion.

The alternating signal of the radio-frequency trap, as previously mentioned, is assumed to be generated by the motion of the metal atom electrons close to the Fermi energy. The electron motion can be traced back to an oscillating electronic cloud that produces an electromagnetic field because of the charge separation due to the oscillation of these electrons relative to the bound lattice ions. A coherent mechanism of these electron cloud oscillations is assumed in the model, such that no phase is subject to random noise as well as in plasmons involving processes.

The adiabatic approximation allows us to consider the Pd atoms, oscillating at acoustic frequency, to be at rest compared with the H or D atoms, which oscillate in the range of the optical frequencies in the metal-H(D) system. The deuteron plasma frequency is about two orders of magnitude lower than the electron plasma frequency,[23,24] so their dynamics is studied assuming that the oscillating electron clouds primarily interact with the deuterons as alternating signals neglecting their proper motion.

Figures 1a and 1b show the Pd lattice cell: The octahedral sites are in the middle between the vertices of the cubic structure; the tetrahedral sites, which should be available for deuterons above $x = \mathrm{H(D)/Pd} = 0.95$ (Ref. 5), belong to the intersection between the (101) and $(10\bar{1})$ planes (see Fig. 1a).

The oscillations of the electron clouds, in principle, can develop, for instance, along one lattice plane like (100), (101), or $(10\bar{1})$. In the following we describe the system such that any oscillation direction can be selected; however, for simplicity's sake, the calculations below have been limited to (100) direction.

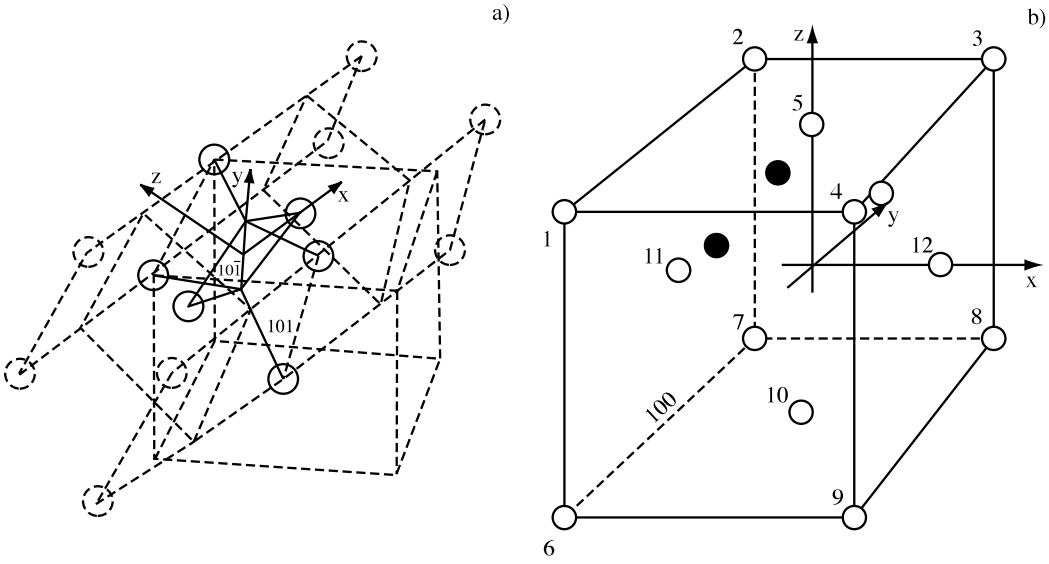

Fig. 1. (a) Palladium (or nickel) lattice cell, intersection of the planes (101) and $(10\bar{1})$. (b) Palladium (or nickel) lattice cell with the system of coordinates.

We can assume, for the system shown in Fig. 1b, that the charges creating the signal along the (100) plane direction belong to atoms 1, 2, 3, 4, and 5 (on the top of the cell) and to atoms 6, 7, 8, 9, and 10 (on the bottom of the cell).

The electron displacements are charge density oscillations producing an alternating electric potential difference that creates an electric field. The direction of the oscillations is, in principle, arbitrary. Therefore, the direction of the oscillating charge is allowed to range between the direction of the *z* axis and the direction of the *x* axis. When the direction of the oscillating charge moves away from one plane, the charge density within that plane decreases and the signal across the plane is also reduced. This effect is taken into account by introducing a factor ranging between 0 and 1 in the peak signal. For instance, if the oscillation develops in the *z* direction, the signal is maximized in the *z*-*y* plane but it is zero in the *y*-*x* plane. To the contrary, if the oscillation develops along the *x* direction the resulting signal is maximum in the *y*-*x* plane, but it is zero in the *z*-*y* plane. The projection of the system in the *z*-*x* plane gives a simplified 2-D view of the spatial oscillations of the electron clouds, as is shown in Figs. 2a and 2b. In the situation described by Fig. 2a, we have the maximum field along the *z* axis (*z*-*y* plane in the 3-D representation) and no field along the *x* direction (*x*-*y* plane in the 3-D representation).

Let E_x and E_z be the effective components for the electric field for the ion dynamics. The value E_y is always zero because the oscillations are assumed to occur between the *z* and *x* directions only, i.e., orthogonal to the *y* axis; thereby, no component of the field develops in such a direction because no separation of charge occurs along the *y* direction.

The aforementioned situation leads to sinusoidally time-varying forces whose strength is proportional to the distance from the origin of the coordinate system.

In the following, a system of two charged particles, moving in the confinement space, is studied; labeling the particles $i = 1,2$, for a particle with mass m_i and charge q_i, the equations of motion under the action of the trap signal and the interaction potential with another charged particle are as follows:

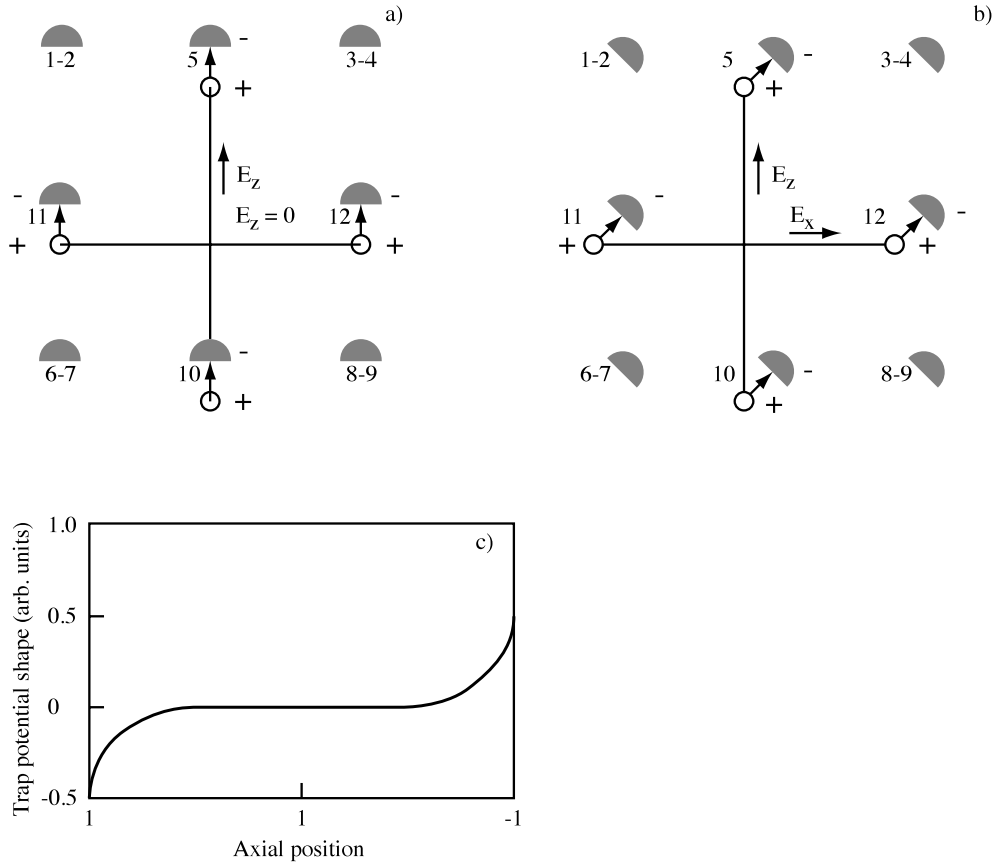

Fig. 2. (a,b) Two-dimensional view of the electronic cloud oscillations. (c) Two-dimensional projection of the potential along a plane.

$$m_i \frac{d^2x_i}{dt^2} = \beta F_{xi}^{Coul} + F_{xi}^{Trap} + F_{xi}^{Damping} \ ,$$

$$m_i \frac{d^2y_i}{dt^2} = \beta F_{yi}^{Coul} + F_{yi}^{Trap} + F_{yi}^{Damping} \ ,$$

and

$$m_i \frac{d^2z_i}{dt^2} = \beta F_{zi}^{Coul} + F_{zi}^{Trap} + F_{zi}^{Damping} \ , \qquad (1)$$

where

x_i, y_i, z_i = coordinates of the particle from the central origin

t = time

$F_{xi}^{Coul}, F_{yi}^{Coul}, F_{zi}^{Coul}$ = components of the Coulomb force acting on the particle, respectively

β = Thomas-Fermi screening factor

$F_{xi}^{Trap}, F_{yi}^{Trap}, F_{zi}^{Trap}$ = components of the trap force, respectively

$F_{xi}^{Damping}, F_{yi}^{Damping}, F_{zi}^{Damping}$ = components of the damping force, respectively.

The damping force is evaluated from the average gradient of the energy barrier[20]; however, for simplicity's sake, this damping will be neglected because this term is a low-weight term that does not produce a significant effect on the particle dynamics.

Then the expressions for the various forces are

$$F_{xi}^{Coul} = q_i q_j \frac{x_i - x_j}{[(x_i - x_j)^2 + (y_i - y_j)^2 + (z_i - z_j)^2]^{3/2}} \ , \qquad (2)$$

$$F_{yi}^{Coul} = q_i q_j \frac{y_i - y_j}{[(x_i - x_j)^2 + (y_i - y_j)^2 + (z_i - z_j)^2]^{3/2}} \ , \qquad (3)$$

and

$$F_{zi}^{Coul} = q_i q_j \frac{z_i - z_j}{[(x_i - x_j)^2 + (y_i - y_j)^2 + (z_i - z_j)^2]^{3/2}} \ , \qquad (4)$$

where $i, j = 1,2$ and $i \neq j$.

An expression for the trap force, produced by the lattice electromagnetic field, can be obtained by assuming that the oscillations of the electron clouds in each plane produce the same effect as an oscillating dipole on the moving particle. This picture, after some tedious but essential calculations, leads to the following expressions for the components of the trap force:

$$F_{xi}^{Trap} = 8(1-\alpha) q_i \rho N e \frac{(l_0^2 + x_i^2)}{(\gamma x_i^2 - l_0^2)^2} \cos(\Omega t) \ , \qquad (5)$$

$$F_{yi}^{Trap} = 0 \ , \qquad (6)$$

and

$$F_{zi}^{Trap} = 8\alpha q_i \rho N e \frac{(l_0^2 + z_i^2)}{(\gamma z_1^2 - l_0^2)^2} \cos(\Omega t) \ , \qquad (7)$$

where

e = electron charge

N = number of oscillating electrons for metal atom

γ = shape factor ($\sim$1) required to avoid the singularity points effect at the trap edges

α = factor ranging between zero and one that accounts for the effect of the oscillation direction on the peak signal in each plane

l_0 = characteristic length of the trap (the distance of the edge from the central origin of the trap)

ρ = factor taking into account the number of atoms that contribute to the signal (typically, the number of atoms on the edges of the confinement space).

Figure 2c shows the shape of the potential along the dipole axis for a certain time within the cell.

The frequency of the alternating signal can be evaluated by considering the oscillating electrons as an ideal electron plasma[24] whose characteristic frequency (electron plasma frequency) is well known as

$$\Omega \cong \frac{e}{m_e^{1/2}} n^{1/2} \approx (10^{15} \div 10^{16} \ \mathrm{s}^{-1}) \ , \qquad (8)$$

where m_e is the electron mass and n is the electron plasma density. In this calculation, it is assumed, as mentioned before, that only the electrons close to the Fermi level participate in the oscillations. Considering that the number of electrons at the Fermi level is close to the density of state at such a level, this number is $\sim$7 per atom in palladium hydride and $\sim$10 per atom in nickel hydride,[32] giving $n \sim 10^{23}$. The corresponding density number of conduction electrons in the transition metals is $\sim 2 \times 10^{23}$.

This description leads to sinusoidally time-varying forces with strengths proportional to the mean distance of the electron cloud from the origin of the coordinate system.

By introducing the dimensionless variables

$$\bar{x} = \frac{x}{l_0} \ , \quad \bar{y} = \frac{y}{l_0} \ , \quad \bar{z} = \frac{z}{l_0} \ , \quad \xi = \frac{\Omega t}{2} \ , \qquad (9)$$

the dimensionless equations of motion read as follows:

$$\frac{d^2\bar{x}_i}{d\xi^2} = 8(1-\alpha)\,\frac{q_i\,\rho Ne}{m_i\,\Omega^2}\,l_0\,\frac{(1+\bar{x}_i^2)}{(\gamma x_i^2 - l_0^2)^2}\cos(2\xi+\psi) + \frac{4q_i\,q_j}{m_i\,\Omega^2}\,\frac{\bar{x}_i-\bar{x}_j}{[(x_i-x_j)^2+(y_i-y_j)^2+(z_i-z_j)^2]^{3/2}}\,\beta\ , \tag{10}$$

$$\frac{d^2\bar{y}_i}{d\xi^2} = \frac{4q_i\,q_j}{m_i\,\Omega^2}\,\frac{\bar{y}_i-\bar{y}_j}{[(x_i-x_j)^2+(y_i-y_j)^2+(z_i-z_j)^2]^{3/2}}\,\beta\ , \tag{11}$$

and

$$\frac{d^2\bar{z}_i}{d\xi^2} = 8\alpha\,\frac{q_i\,\rho Ne}{m_i\,\Omega^2}\,l_0\,\frac{(1+\bar{z}_i^2)}{(\gamma z_i^2 - l_0^2)^2}\cos(2\xi+\psi) + \frac{4q_i\,q_j}{m_i\,\Omega^2}\,\frac{\bar{z}_i-\bar{z}_j}{[(x_i-x_j)^2+(y_i-y_j)^2+(z_i-z_j)^2]^{3/2}}\,\beta\ , \tag{12}$$

where the random phase ψ has been introduced to account for the signal phase when the shot particle enters the system.

The differential equations (10), (11), and (12) describe the dynamics of one or two particles in the trap, within the framework of the proposed description and assumption already cited.

We mentioned in Sec. I that even if both particles can be considered in motion from the beginning of the analysis (initial conditions), it is of interest to assume that one of them, the target, is at rest (e.g., in a tetrahedral site), while the moving one enters the trap with a random energy (close to thermal since it can be considered entering the system by diffusion) as well as random position and direction. In such a way, the number of particles that produce an effective interaction (minimum distance between the particles on the order of 0.1 Å or less in order to have a possible overlapping of the two nucleus wave functions) can be evaluated by a Monte Carlo calculation.

The calculation shows, however (see the following) that a charged particle moving in the trap can reach an energy of some thousands of electron volts. This energy gain is equivalent to the particle gaining thousands of photons from the lattice trap because the electromagnetic signal frequency is $\sim 10^{16}$ s^{-1} and hence the photon energy is ~10 eV; the individual photon contribution can be considered small, and we can assume that the exchange of energy is a nonperturbative continuous process. Thus, a classical description of the particle dynamics is possible.

Then within this framework, the dynamics of the moving particles is described by a numerical solution of the system of differential equations (10), (11), and (12).

III. DYNAMICS ANALYSIS: RESULTS

The numerical solution of the system of differential equations (10), (11), and (12) has been carried out using initial conditions described earlier. This study concerns interactions between two deuterons within a Pd lattice, one moving under the trap force action and the other assumed to be at rest within a tetrahedral site. In this calculation, the electron-cloud oscillation direction is assumed to be approximately oriented along the *z*-*y* plane direction ($\alpha \cong 0.995$).

The electrons are approximated by an ideal plasma, the frequency being treated as a parameter ranging between 5×10^{15} and 10^{16} (1/s), namely, close to the ideal electron plasma frequency [see Eq. (8)].

As already mentioned, the initial energy of the incoming shot particle is chosen randomly within the range from 0.02 to 0.03 eV, close to thermal. Thus, the initial velocity components do not modify the dynamics because of the dominant role of the trap force in the dynamics.

The initial position and direction of motion of the moving particle could be given randomly within a Monte Carlo calculation. However, since we are interested in a collision event, to save computational time, the initial position and direction of the incoming shot are selected to cause the shot particle to closely approach the target [i.e., $\bar{x}_1(t=0)=0.5$, $\bar{y}_1(t=0)=0.5$, $\bar{z}_1(t=0)=1$; $\bar{x}_2(t=0)=0.5$, $\bar{y}_2(t=0)=0.5$, $\bar{z}_2(t=0)=0$]; the particles are aligned with the main direction of the electric field. Figure 3a shows the evolution of the distance between the shot and the target for these initial conditions with an electron plasma frequency $\Omega = 10^{16}$ (1/s). We can see that the distance decreases to ~0.085 Å

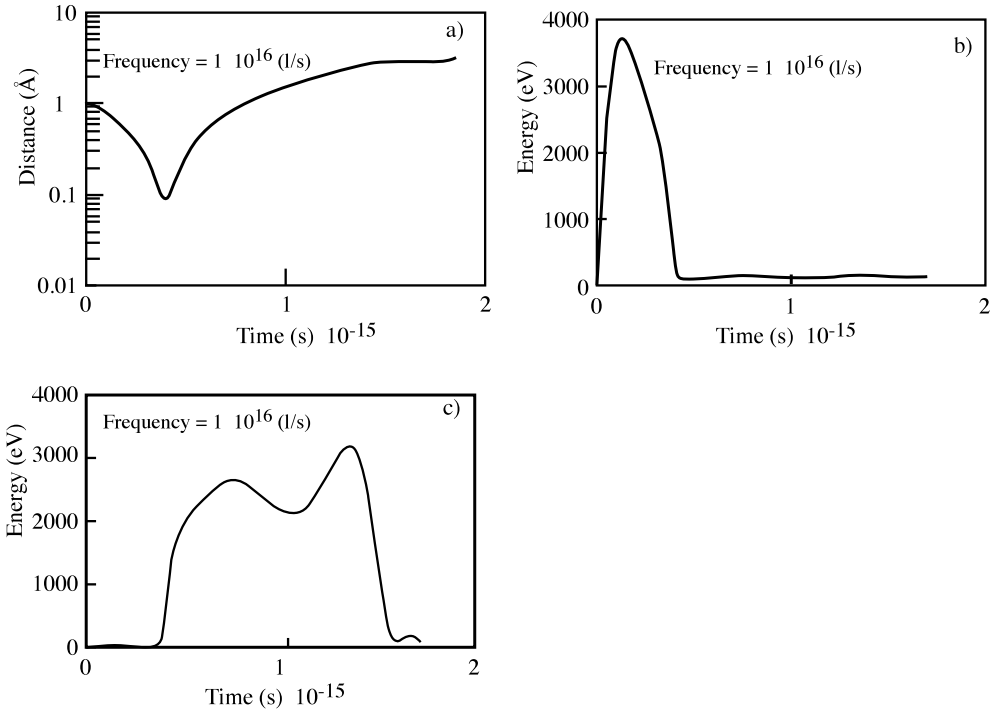

Fig. 3. (a) Evolution of the distance between two deuterons in the Pd lattice when the initial conditions produce a collision effect (electron plasma frequency 10^{16} (1/s). (b) Evolution of the shot particle energy. (c) Evolution of the target particle energy.

(distance of closest approach) and then increases again. Figure 3b shows the evolution of the shot energy: It can be seen that although the initial energy is within the thermal range, the particle can gain some kilo-electron-volts of energy because of the acceleration due to the action of trap force. Figure 3c shows the evolution of the target particle energy after the closest approach. A similar trajectory has been also obtained within a Monte Carlo loop by using a large enough number of particles (see the following) to reproduce initial conditions quite similar to those aforementioned.

Figure 4a shows the evolution of the distance between shot and target with the same initial conditions of the previous case but with $\Omega = 5 \times 10^{15}$ (1/s). We can see that the effect of the decreased frequency is that the minimum distance of approach decreases to 0.05 Å, so the collision becomes more effective because the shot gains a larger energy, as shown in Fig. 4b. This

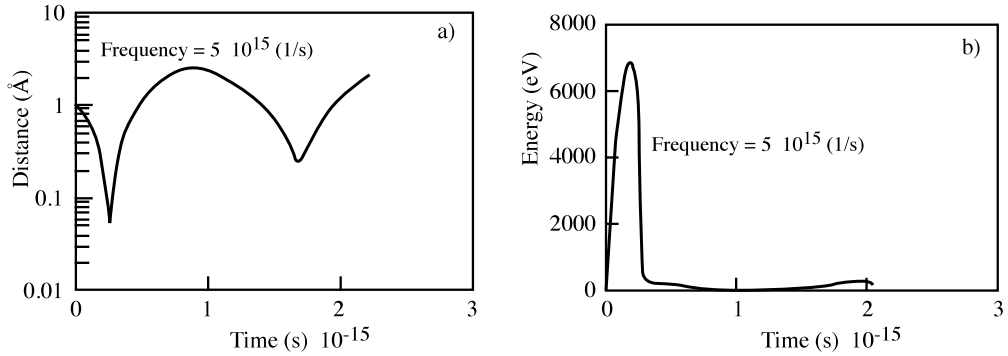

Fig. 4. (a) Evolution of the distance between two deuterons in the Pd lattice when the initial conditions produce a collision effect (electron plasma frequency) 5×10^{15} (1/s). (b) Evolution of the shot particle energy.

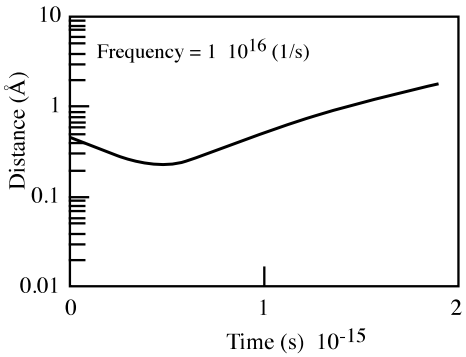

Fig. 5. Evolution of the distance between two deuterons in Pd when the initial conditions do not produce the collision effect.

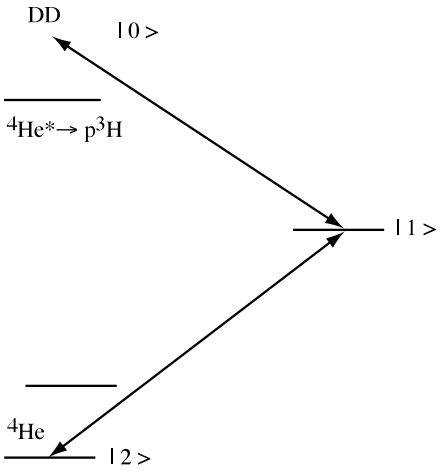

Fig. 6. Nuclear decay synoptic.

behavior is due to the fact that when the flight time of the shot particle becomes quite similar to the oscillation period, the shot is less affected by the decelerating force following the time of the closest approach. Energy conservation requires that the kinetic energy exchanged for Coulomb potential energy is just the difference between the energy of the shot before the collision and the energy of the target after the collision. This difference of energy is proved to typically range between 1 and 2 keV for the head collisions that occur with the initial conditions selected.

A Monte Carlo–based simulation was carried out on the basis of the random initial conditions for the shot particle to evaluate the percentage of passes by the shot past the target that can be taken as a collision according to the meaning explained previously. Assuming any pass with an approach below 0.1 Å to be a collision event (the energy gained by the shot is then of some kilo-electronvolts), it was estimated that approximately five shot particles out of 1×10^5 produce collision with the deuteron at rest within a tetrahedral site.

Figure 5 plots the distance between the two deuterons as a function of time in the Pd lattice for the case where the initial conditions are different for those previously selected to produce a collision event (i.e., the particle enters the confinement region from a position that is close to an octahedral position).

IV. THE ^{4}He* DECAY

IV.A. Background

In this section, the effect of the electric field on the nuclear decay of an excited ^{4}He produced through a D-D reaction is considered.

The effect of the lattice electromagnetic field on the probability amplitude of an excited-to-ground state decay of the ^{4}He* nucleus has already been studied in the literature[16] through the interaction potential given by the product between the nuclear current and the field potential vector. The coupling between the excited ^{4}He nucleus and the lattice assumes the same lattice and field parameters used for the analysis of the ion dynamics. According to the idealized level scheme of Fig. 6, the study shows that the dynamics is controlled by the transition $0 \rightarrow 1$, taking into account the effect of the electromagnetic field on the reaction channel.

The following uses a single-particle approximation in the calculation of the nuclear electrical current. The electromagnetic lattice field amplitude is evaluated on the basis of the charge separation, due to the plasmons, as explained in Sec. III concerning ion dynamics.

The transition matrix elements are calculated taking into account the coupling between the nuclear current of the excited nucleus and external field due to the lattice electron cloud oscillations. The nuclear current in the excited nucleus is considered to be created by the motion of a single particle (proton).

One aim of this work is to investigate the effect of the lattice field on both the dynamics of the ions embedded in the lattice and the nuclear decay of the compound ^{4}He* nucleus.

The energy released by the excited nucleus is supposed to be given, with a nonradiative process, to a region of the lattice defined by the coherent behavior of the plasmons (i.e., of the electromagnetic field created by the oscillating electrons). The size of such a domain can be approximately estimated by[33]

$$\lambda = \frac{2\pi c}{\Omega} \approx 1000 \text{ Å} \ , \qquad (13)$$

where c is the velocity of the light.

The decay energy is then distributed over a very large volume of the lattice in comparison with the atomic size; therefore, such a volume can be considered as an infinite reservoir that is not damaged or dramatically modified by the energy transfer and that recoil the energy as a whole.

A fast transition is allowed because the decay is considered to take place through an electromagnetic coupling between the excited nucleus and the electromagnetic field of the lattice coherence domain.

The excited alpha particle cooling to the ground state (^{4}He) is mediated in the proposed picture by the Fermi electrons, participating with the plasmons, that release the acquired electromagnetic energy toward the phonons of the lattice and low-energy radiation emission (X rays).

According to the semiclassical approximation and by considering the coherence domain as an infinite reservoir, if we can assume that the distribution of the electromagnetic field is not strongly affected over the coherence domain by the excited nucleus decay, then the computation of the matrix element is carried out by means of the nucleus wave function in the initial and final states.

The basic idea is to make an evaluation of the effect of the field in the lattice on the nuclear reaction D+D in analogy with the internal conversion process. Then, by assuming that in the lattice, because of the electromagnetic field the product is ^{4}He* without γ emission, we first estimate a stimulated transition probability (to verify that there is a nonzero probability for such a transition), and then we compare the decay probability for the stimulated transition both with the probability for a *d*-wave ($E2$) gamma decay process and also with the probability of the two main channels for the traditional D-D reaction (i.e., D + D $\rightarrow p$ + T and D + D $\rightarrow n$ + ^{3}He) .

IV.B. Interaction Between the Excited Nucleus and the Electromagnetic Field

Let us consider a particle of charge e moving in an electromagnetic field. The electric and magnetic field strengths can be expressed in terms of the vector and scalar potentials $\vec{A}(\vec{r},t)$ and $\varphi(\vec{r},t)$ respectively:

$$\vec{E} = -\nabla\varphi - \dot{\vec{A}} \tag{14}$$

and

$$\vec{B} = \vec{\nabla} \wedge \vec{A} \ . \tag{15}$$

The classical Hamilton function relative to the particle motion is given as

$$H = \frac{1}{2m}(\vec{p} - e\vec{A})^2 + e\varphi \ , \tag{16}$$

where $\vec{p}$ is the generalized momentum.

This formulation indicates the simplest way of coupling the electric field to the motion of the particle. The momentum $\vec{p}$ is replaced by the term $\vec{p} - e\vec{A}$. The substitution $\vec{p} - e\vec{A}$ is gauge invariant and is called minimal coupling.[34] Hamilton's canonical momentum $\vec{p}$ is the sum of the kinetic momentum $m\vec{v}$ and the term $e\vec{A}$, which is determined by the vector potential.

The transition to quantum mechanics is obtained by replacing the canonical momentum $\vec{p}$ by $(\hbar/i)\vec{\nabla} - \vec{A}e$, according to the rules of quantization in the present coordinates.

Thus, the Hamiltonian becomes

$$\hat{H} = \frac{1}{2m}\left(\frac{\hbar}{i}\vec{\nabla} - \vec{A}e\right)^2 + e\varphi \ . \tag{17}$$

Neglecting the contribution from the scalar vector and considering the Coulomb gauge ($\nabla\cdot\vec{A} = 0$), we obtain the following Hamiltonian operator:

$$\hat{H} = \hat{H}_0 + \hat{H}_I \ , \tag{18}$$

where the terms on the right side of Eq. (18) represent the unperturbed and interaction parts of the Hamiltonian, respectively. Thus,

$$\hat{H}_0 = \hat{p}^2/(2m) \ . \tag{19}$$

If the electromagnetic field is assumed to be a plane wave,

$$\varphi = 0 \ , \quad \vec{A} = \vec{A}_0 \sin(\vec{k}\cdot\vec{r} - \Omega t) \ , \tag{20}$$

Eq. (18) leads to a stimulated transition.

If we limit ourselves to the interaction of the charge with the electromagnetic lattice field, the interaction term H_I becomes simply

$$\hat{H}_I = \frac{e}{m}\hat{p}\vec{A} \ . \tag{21}$$

In the absence of the electromagnetic field, the wave function of the particle satisfies the Schrödinger equation with Hamiltonian H_0. The ground state is a stationary state because the higher states can radiate spontaneously and change their configuration.

It is easily verified that the effect of the magnetic field in the lattice confinement space is negligible compared to that of the electric field. Then, from Eq. (14) it follows that

$$\vec{E} = \Omega\vec{A}_0 \cos(\vec{k}\cdot\vec{r} - \Omega t)$$

and

$$\vec{B} = \vec{k} \wedge \vec{A} \cos(\vec{k}\cdot\vec{r} - \Omega t) \ . \tag{22}$$

In the problem under study, the potential vector refers to an electric field with components oriented in the directions of the planes *y*-*z* and *x*-*z* that are mutually orthogonal. Then, in particular when the oscillations of the electron clouds develop along the *z* axis within the *z*-*y* plane, the potential vector becomes

$$\vec{A}(z,t) = \vec{A}_0 e^{\pm ikz - i\Omega t} \ . \tag{23}$$

The remaining problem is to evaluate the transition probability of the nucleus from the initial state (excited) to the final one under the effect of the field created in the lattice by the electron oscillations.

With reference to Fig. 6, the state at a time t can be assumed to be represented by the overlapping of three states:

$$|\Psi(t)\rangle = C_0(t)e^{-i\omega_0 t}|0\rangle + C_1(t)e^{-i\omega_1 t}|1\rangle + C_2(t)e^{-i\omega_2 t}|2\rangle \ , \tag{24}$$

where ω_0, ω_1, and ω_2, are the energies (in units of $\hbar$) of the respective energy levels of Fig. 6.

The coefficients $C_{0,1,2}$ are obtained from the Schrödinger equation

$$i\hbar \frac{\partial}{\partial t}|\Psi\rangle = (H_0 + A\cdot J)|\Psi\rangle \tag{25}$$

through the usual iterative procedure, according to the initial conditions

$$C_0(0) = 1 \ , \quad C_1(0) = C_2(0) = 0 \ . \tag{26}$$

Then considering that $\langle 2|H_I|0\rangle = 0$, we obtain

$$C_0(t) = 1 \ , \tag{27}$$

$$C_1 = \frac{a}{\hbar(\omega_0 - \omega_1)}\left[e^{-i(\omega_0-\omega_1)t} - 1\right] \ , \tag{28}$$

and

$$C_2 = -i\frac{ab}{\hbar(\omega_0-\omega_1)} \times \left\{ \frac{1}{-i\hbar(\omega_0-\omega_2)}\left[e^{-i(\omega_0-\omega_2)t} - 1\right] - \frac{1}{-i\hbar(\omega_1-\omega_2)}\left[e^{-i(\omega_1-\omega_2)t} - 1\right]\right\} \ , \tag{29}$$

where

$$a \equiv \langle 1|\hat{H}_I|0\rangle \tag{30}$$

$$b \equiv \langle 2|\hat{H}_I|0\rangle \ . \tag{31}$$

Further, we can assume that

$$\omega_0 - \omega_1 \cong \omega_1 - \omega_2 \Rightarrow \omega_0 - \omega_2 = 2(\omega_0 - \omega_1) = 2(\omega_1 - \omega_2) \ . \tag{32}$$

Note that the probability amplitude is controlled by the $|0\rangle \rightarrow |1\rangle$ transition since $C_1 > C_2$; in fact, $C_1 \propto a$ while $C_2 \propto a\cdot b \approx a^2$.

Now we can evaluate the transition probability. Let T be the characteristic time of the process (see the following), the interaction time between the decaying nucleus and the lattice electromagnetic field. Then the amplitude of the transition matrix element is

$$a_{f,i} = -\frac{i}{\hbar}\int_{-\infty}^{T} \langle f|\hat{H}_I|i\rangle \, dt \ , \tag{33}$$

where

$$\langle f|\hat{H}_I|i\rangle = \langle 0|\hat{H}_I|0\rangle e^{-i\omega_0 t} + aC_1^*(t)e^{-i\omega_0 t} + \langle 2|\hat{H}_I|0\rangle C_2^* e^{i(\omega_2-\omega_0)t} \ , \tag{34}$$

which, being the first and the last term in the right side zero, becomes

$$\langle f|\hat{H}_I|i\rangle = aC_1^* e^{i(\omega_1-\omega_0)t} \ . \tag{35}$$

Therefore, in view of expression (33), we obtain

$$a_{fi} = -\frac{i}{\hbar}\int_0^T \frac{a^2}{\hbar(\omega_0-\omega_1)}(e^{-i(\omega_1-\omega_0)t} - 1)e^{i(\omega_1-\omega_0)t}\, dt \ . \tag{36}$$

Then,

$$a_{fi} = \frac{i}{\hbar^2}\frac{a^2}{(\omega_0-\omega_1)}\left[\frac{1}{(\omega_1-\omega_0)}(e^{i(\omega_1-\omega_0)T} - 1) - iT\right] \ , \tag{37}$$

and

$$T \cong \frac{1}{(\omega_0-\omega_1)} \ . \tag{38}$$

It can also be easily demonstrated that an increasing interaction time enhances the value of the transition probability; consequently, a reasonable approximation expression for the matrix element is

$$a_{fi} \cong \gamma[(\cos(\omega_{10}T) - 1) + i(\sin(\omega_{10}T) - 1)] \ , \tag{39}$$

where

$$\gamma = -\frac{1}{\hbar^2}\frac{a^2}{(\omega_0-\omega_1)^2} \tag{40}$$

$$\omega_{10} = \omega_0 - \omega_1 \ . \tag{41}$$

The square module then is

$$|a_{fi}|^2 \cong \gamma^2[3 - 2(\cos(\omega_{10}T) + \sin(\omega_{10}T))] \ . \tag{42}$$

Taking into account that

$$\langle 1|\hat{H}_I|0\rangle = \frac{eA_0}{m}\langle 1|\hat{p}|0\rangle \ , \tag{43}$$

from

$$\hat{p} = m\frac{d\hat{r}}{dt} \tag{44}$$

and

$$i\hbar \frac{d\hat{r}}{dt} = [\hat{r}, \hat{H}] \ , \tag{45}$$

we find that

$$\langle 1|\hat{p}|0\rangle = \frac{1}{i\hbar} m\langle 1|\hat{r}H - H\hat{r}|0\rangle$$
$$= im(\omega_1 - \omega_0)\langle 1|\hat{r}|0\rangle \ . \tag{46}$$

Then

$$a = 5 \times 10^{-14}$$
$$|a_{fi}|^2 \cong 10^{-6}\{3 - 2[\cos(\omega_{10}T) + \sin(\omega_{10}T]\}$$
$$> 10^{-6} \ , \tag{47}$$

so that the considered range of frequencies results in

$$\Omega = 10^{15} \text{ s}^{-1} \Rightarrow |a_{fi}|^2 > 10^{-3} \ ;$$
$$\Omega = 10^{16} \text{ s}^{-1} \Rightarrow |a_{fi}|^2 < 10^{-5} \ .$$

Now, on the basis of this result, a preliminary estimate of the decay probabilities of the compound state into the possible channels is possible.

The D-D reaction, in vacuum, has two equiprobable main reaction channels, i.e., $D(d,p)T$ and $D(d,n)^3He$, with a branching ratio of ~50% and a ^4He production channel $D(d,\gamma)^4He$ with a small branching ratio ($\leq 10^{-7}$) (Ref. 35). The energy for the emitted gamma is 23.8 MeV.

This picture suggests the possibility of another channel for the reaction in the condensed matter, which is an electromagnetic stimulated transition with a nonradiative release of energy to the coherence domain (the infinite reservoir).

The probability P_i of a decay of a compound state into a generic channel i is given by[36]

$$P_i = \frac{\Gamma_i}{\Gamma} \ , \tag{48}$$

where Γ_i is the appropriate partial width and Γ is given by

$$\Gamma = \sum_i \Gamma_i . \tag{49}$$

For the traditional $D(d,p)T$, $D(d,n)^3He$ channels, the partial width for either [e.g., Γ_n for $D(d,n)^3He$] suggests a nearly equal branching ratio of 50%. The maximum value of the width is given by[37,38]

$$\Gamma_{(D,n)}^{max} = k_n R_N \frac{\hbar^2}{m_n R_N^2} \ , \tag{50}$$

where

k_n = center-of-mass wave number of channel $n + {}^3He$ ($m_n v_n/\hbar$)

R_N = nuclear radius of the compound nucleus [3×10^{-15} m (Ref. 35)]

m_n = neutron mass

v_n = neutron velocity.

The resulting value for $\Gamma_{(D,n)}^{max}$ ($\sim 10^{-13}$) is close to the limit given by the uncertainty principle so that an approximate evaluation for $\Gamma_{(D,n)}$ can be carried out on the basis of a comparison between the cross sections (deprived of the Gamow term) of the $D(D,n)^3He$ reaction and of the D-D reaction in the metal lattice.

To have a rough estimate of the electromagnetic stimulated transition cross section, we can apply the well-known relationship for σ_{st} using the principle of the detailed balance[35,39,40]:

$$\sigma_{st} \approx \frac{8\pi^3 \nu_{fi} V_N |a_{fi}|^2}{c} \ , \tag{51}$$

where ν_{fi} ($\cong 10^{21}$ s^{-1}) is the decay frequency and V_N is the volume of the nucleus. The transition matrix element a_{fi} can be obtained by taking into account the coupling with the lattice electromagnetic field, properly normalizing the energy to $\hbar/R_N m$ (Ref. 35) (that is on the order of $\hbar\omega_{10}$).

The calculations and the literature data give, for a frequency of the electromagnetic field on the order of 10^{15} (s^{-1}) for a field peak value on the order of 10^{13} (V/m) (that is not far from the value calculated by the plasmon theory) and with an exchange energy of 1 keV, the following result:

$$\chi = \frac{\sigma_{(D,n)}}{\sigma_{st}} \approx 10^{-4} \ . \tag{52}$$

So we can assume the width for the stimulated transition to be very close to the limit given by the uncertainty principle ($\Gamma_{st} = \Gamma^{max}$) and

$$\Gamma_{(D,n)} = \chi \Gamma_{st} \ . \tag{53}$$

The gamma emission channel width can be estimated by means of the well-known relationship for an electric quadrupole decay

$$\Gamma_\gamma = 4.8 \times 10^{-8} E_r^5 A^{4/3} \ , \tag{54}$$

or we can assume that the vacuum channel probability ratio between the gamma emission and the (D,n), (D,p) channel maintains.

The computation leads to $P_{st}(=1) \gg P_{(D,n)} \gg P_{(D,\gamma)}$, so that the nonradiative stimulated decay process becomes the dominant one in the lattice when a proper electromagnetic signal is given by the lattice. This result,

which in any case, as we stated previously, because of the simplifications done, has to be considered as indicative, is in reasonable accordance with the experimental results where neutrons and gamma rays have not been significantly observed above the natural background.[41,42]

V. EXCESS OF HEAT PRODUCTION: ESTIMATION

In the majority of cold fusion calorimetric experiments, studying the Pd-D system, an excess of heat production has been observed ranging between some tenths of watts for cubic centimetres up to some hundreds of watts for cubic centimetres of cathodes.[43] We have seen, in the aforementioned study, that there is an interesting collision effect between deuterons embedded within a Pd lattice. The simulation suggests that ~1 collision occurs over 10^4 to 10^5 (depending on the frequency of the signal) particles entering a lattice with a target staying at rest in the tetrahedral sites. Also, the deuterons can gain an energy of some kilo-electron-volts due to acceleration by the lattice trap field.

In Sec. IV we have seen the effect of the lattice electromagnetic field on the reaction channel with respect to the reaction in vacuum. Now, to roughly estimate the order of magnitude of the effects involved, we consider the system of fusionable deuterons in the lattice when the aforementioned collision dynamics takes place. As first approximation, we assume that on the microscopic scale of the sublattice, where the collision occurs, the reactivity of the deuterons can be approximated with the reactivity in the vacuum (because of the very small scale ion dimensions in comparison to the lattice separation distance); however, a different decay channel is assumed for the compound nucleus, in accordance with the aforementioned results. This is thought to be a conservative hypothesis because several experimental results[44,45] show that there is an enhancement of the reaction cross section in condensed matter.

Within this framework, the deuterons can be considered to fall into two different populations: one at rest within the tetrahedral sites (low energy) and the other with higher energy (the shots). The reaction rate is

$$R = n_{D1} n_{D2} \langle \sigma v \rangle \ , \tag{55}$$

where n_{D1} and n_{D2} are the number density of shot (i.e., the deuterons diffusing toward the tetrahedral sites) and of the deuterons at rest within the tetrahedral sites, respectively (it is of interest to highlight that a nonequilibrium condition is required for the excess of heat production to occur.[4]) Furthermore, σ is the relevant fusion cross section, v the relative velocity, and $\langle \sigma v \rangle$ is the average of the product over some appropriate velocity distribution function (reactivity).

For the thermodynamic reasons previously mentioned, when the D/Pd atomic ratio is close to one, the density of the deuterons staying in the tetrahedral sites can be considered to be equal to the order of the deuteron density within the lattice ($N_0 = 6.8 \times 10^{22}$); then $n_{D2} \approx 10^{22}$ cm^{-3}. In the previous analysis, the deuterons were assumed to enter the lattice cell by diffusion. Then the number of the particles that can participate in the dynamics is roughly equal to the particles that can overcome the diffusive activation energy barrier E_b between the octahedral and tetrahedral sites: $E_b = 0.32$ eV (Ref. 46). Therefore, the density of the deuterons that can move by diffusion toward the tetrahedral sites is $N_0 \exp(-E_b/kT)$, while the density number of fusionable nuclei entering the trap is $n_{D1} = \Theta N_0 \exp(-E_b/kT)$, where Θ is the probability to have a collision for a deuteron entering the trap ($10^{-4} \div 10^{-5}$, obtained by means of the Monte Carlo calculation as noted earlier). Then, in the proposed picture, only a small fraction of the deuterons embedded in the metal lattice move toward the tetrahedral sites and gain energy from the system. It can be easily evaluated that the energy gained by the fraction of the particle moving toward the tetrahedral sites is just a fraction of the energy involved in the process; furthermore, only a fraction in the range 10^{-4} to 10^{-5} of the particles moving around the tetrahedral sites produce a collision.

For a Maxwellian distribution, the reactivity[47] of the D-D reaction can be approximated by the following:

$$\langle \sigma v \rangle = 1.0 \exp\left(\frac{a_1}{T^r} + a_2 + a_3 T + a_4 T^2 + a_5 T^3 + a_6 T^4 \right) \quad (\text{cm}^3/\text{s}),\ T\ (\text{keV}) \ , \tag{56}$$

where

$$a_1 = -15.511891$$
$$a_2 = -35.318711$$
$$a_3 = -0.012904737$$
$$a_4 = 0.00026797766$$
$$a_5 = -0.0000029198685$$
$$a_6 = 0.000000012748415$$
$$r = 0.3735.$$

(In our case, a narrow Maxwellian distribution can be assumed due to the effect of the random initial condition and signal phase on the shot energy.)

Figure 7 shows the behavior of the excess heat production for an increasing temperature, assuming that the product of the D-D reaction is excited ^{4}He and that the energy produced by a reaction is 23.8 MeV .

In the following, a preliminary study of the direct decay of excited ^{4}He (^{4}He*) along with transfer of the excitation energy to the lattice (i.e., providing excess heat) is considered.[16–18,48]

The calculations have been done by considering three values for the energy of the impinging particle (1.1, 1.5, and 2 keV). A range between 300 and 350 K is taken for

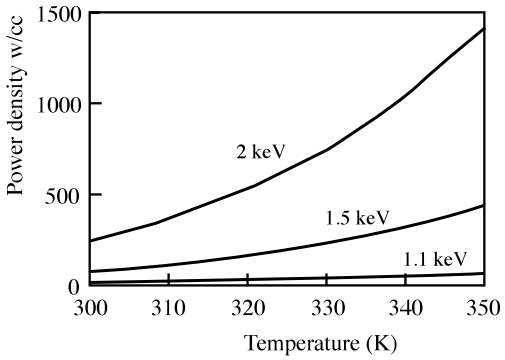

Fig. 7. Behavior of the excess heat production with increasing temperature for three different values of the Coulomb exchanged energy.

the temperature because the cathode temperature is typically higher than the temperature of the electrolyte, particularly when the excess heat occurs. The calculations show a correlation between temperature of the D-loaded sample and the amount of produced excess heat due to the increasing number of fusionable particles with increasing temperature (see the relationship for n_{D1}). This effect has been experimentally demonstrated by Fleischmann et al.[49–53] Further, despite the various approximations introduced in the calculations, the results seem to be in rough agreement with the experimental data that range between 0.1 W/cm^3 up to several hundreds of watts per cubic centimetre (Ref. 33).

A further rough estimate of the power density produced by the D-D reaction for a *d*-wave process in Pd can be done by assuming that the particles' population limiting the process are the diffusing particles. A comparison with the previous estimate will be done. Applying the same relationship of Ref. 16 and taking into account the fraction of particles having proper initial conditions to produce a collision (i.e., is the population limiting the process), we obtain

$$\Pi = \Theta N_0 \exp(E_b/kT)|a_{fi}|^2 \nu_{fi} \exp(-2G_2)\Delta E \ , \quad (57)$$

where

Π = power density

ν_{fi} = decay process frequency ($\cong 10^{22}$ 1/s)

G_2 = Gamow factor for a *d*-wave process [G_2(1.1 keV) = 21.1, G_2(1.5 keV) = 19.11, G_2(2 keV) = 17.2] accounting for the electrostatic effect (as well as Ref. 35)

ΔE = energy for reaction (3.95×10^{-12} J).

The calculations have been done for exchanged Coulomb potential energy values of 1.1, 1.5, and 2 keV and for two different temperatures of 300 and 350 K. The results are summarized in Table I.

TABLE I

Power Density Values (W/cm^3)*

Temperature (K)	1.1 keV (W/cm^3)	1.5 keV (W/cm^3)	2 keV (W/cm^3)
300	0.95 (13)	68 (67)	2100 (260)
350	5.53 (76)	400 (394)	12000 (1520)

*Values in parenthesis refer to the previous estimate.

The difference between the results at low energy is mainly due to the optimistic approximation in the previous calculations to an *s*-wave process reactivity. The *d*-wave calculation shows an upper limit for the power density on the order of 10 kW/cm^3 that has been obtained in some experiments. However, the obtained values, taking into account that all the results have to be assumed as indicative, are in rough accordance with the experimental results.

This picture allows us to consider that if the diffusing particles going toward the reacting zone (i.e., tetrahedral sites) are the limiting population for the reactivity, a temperature increase, even if it could reduce the concentration of the deuterons in the lattice, should, however, increase the number density of the particles producing collisions; then the reactivity could remain significant.

VI. CONCLUSIONS

The model shows that the signal created by the charge density oscillations around the metal atoms produces interesting trajectories of deuterons within the metal lattice. The proposed trap signal shape can produce, with proper initial conditions, an interesting approach mechanism between deuterons in metals like Pd or Ni (the energy gained by the ions in the lattice during their dynamics can partially explain the X-ray emission in the experiments[54]).

The combined effects of the trap force, electrostatic interaction, and nonlinearity give, under proper initial conditions, an interesting collision effect between the particles: During the dynamics, the particles approach one another at a distance that is below their average distance into the lattice.

Even if the distances between the particles have to be considered as indicative because of the approximations previously mentioned, the minimum distance is of the order of a fraction of an angstrom, then a nuclear interaction between nuclei cannot be excluded.

The conditions to have collisions are a D atomic fraction close to one in the metal and coherent oscillations of the Fermi-energy electrons. A high loading ratio is required both to allow the ions to move toward the sublattice and to ensure an appropriate electron density at the Fermi level. The coherent behavior of the electrons has been observed and studied near metal/electrolyte (or metal/gas) interfaces.[25–28] It has also been clarified that the formation of surface electromagnetic waves can be enhanced by surface roughness.

In conclusion, we have to consider that the condition for close approach between two particles is produced by proper values of the electron plasma density, lattice cell geometry, and lattice state. In principle, it is not impossible that a similar behavior could be obtained by using host metals different from Pd and Ni.

The proposed mechanism is a bulk mechanism that can take place also within a region very close to the surface (on the order of hundreds or thousands of angstroms from the metal surface).[25,26]

From the time scale of the phenomenon, we can observe that the approximation of considering the metal atoms at rest is reasonable, because the time scale of the approach between ions in the metal is several orders of magnitude less than the oscillation period of the Pd atoms.

Within the framework of the proposed model, a close approach between protons or deuterons and the host lattice atoms cannot be excluded if the initial conditions are suitable for that, even if a screening mechanism, different from the Thomas-Fermi one, is required[17] to have a reaction.

The shape of the potential in the lattice cell allows us to evaluate that a strong electric field gradient is also present in the system, which could have some effect on the nuclear phenomena.[55]

The study of the effect of the lattice field, on a microscopic scale, on the nuclear process shows a possible shift in the D-D reaction channel.

Therefore, a strong lattice electromagnetic field, able to produce effective collisions between the deuterons, could also be responsible for a significant modification in the decay of the excited nucleus formed by the D-D interaction within the lattice.

The parametric study reveals that an important role is played by A_0 (ratio between the electromagnetic signal amplitude and the electromagnetic signal frequency) since increasing such a parameter produces both an increase in the collision effect and an increase in the transition probability of the nonradiative decay.

ACKNOWLEDGMENTS

The authors are grateful to C. Sibilia, La Sapienza University of Rome (Italy) and to L. Pieroni, ENEA Frascati Research Center (Italy) for the useful hints given to improve the paper.

REFERENCES

1. M. FLEISCHMANN and S. PONS, "Electrochemically Induced Nuclear Fusion of Deuterium," *J. Electroanal. Chem.*, **261**, 301 (1989).

2. K. KUNIMATSU, N. HASEGAWA, A. KUBOTA, N. IMAI, M. ISHIKAWA, H. AKITA, and Y. TSUCHIDA, "Deuterium Loading Ratio and Excess Heat Generation During Electrolysis of Heavy Water by a Palladium Cathode in a Closed Cell Using a Partially Immersed Fuel Cell Anode," *Proc. 3rd Int. Conf Cold Fusion*, Nagoya, Japan, October 20–25, 1992, p. 31.

3. M. C. H. McKUBRE, S. CROUCH-BAKER, A. M. RILEY, S. I. SMEDLY, and F. L. TANZELLA, "Excess Power Observation in Electrochemical Studies of the D/Pd System; The Influence of Loading," *Proc. 3rd Int. Conf. Cold Fusion*, Nagoya, Japan, October 20–25, 1992, p. 5.

4. M. McKUBRE, "Concerning Reproducibility of Excess Power Production," *Proc. 5th Int. Conf. Cold Fusion*, Monte Carlo, Monaco, April 9–13, 1995, p. 5.

5. R. A. ORIANI, "The Physical and Metallurgical Aspects of Hydrogen in Metals," *Trans. Fusion Technol.*, **26**, 235 (1994).

6. F. DE MARCO, A. DE NINNO, A. FRATTOLILLO, A. LA BARBERA, F. SCARAMUZZI, and V. VIOLANTE, "Progress Report on the Research Activities on Cold Fusion at ENEA Frascati," *Proc. 6th Int. Conf. Cold Fusion*, Toya, Japan, October 13–18, 1996, p. 145.

7. A. DE NINNO, A. LA BARBERA, and V. VIOLANTE, "Selection of Palladium Metallurgical Parameters to Achieve Very High Loading Ratios," *Proc. 6th Int. Conf. Cold Fusion*, Toya, Japan, October 13–18, 1996, p. 192.

8. A. DE NINNO, A. LA BARBERA, and V. VIOLANTE, "Deformations Induced by High Loading Ratios in Palladium-Deuterium Compounds," *J. Alloys Compounds*, **253–254**, 181 (1997).

9. A. DE NINNO, A. LA BARBERA, and V. VIOLANTE, "Consequences of Lattice Expansive Strain Gradients on Hydrogen Loading in Palladium," *Phys. Rev. B*, **56**, *5*, 2417 (1997).

10. G. H. MILEY, G. NARNE, M. J. WILLIAMS, J. A. PATTERSON, J. NIX, D. CRAVENS, and H. HORA, "Quantitative Observation of Transmutation Products Occurring in Thin Film Coated Microspheres During Electrolysis," *Proc. 6th Int. Conf. Cold Fusion*, Toya, Japan, October 13–18, 1996, p. 629.

11. B. L. CAIN, A. B. CHENEY, J. M. RIGSBEE, R. W. CAIN, and L. S. McMILLIAN, "Thermal Power Produced Using Thin-Film Palladium Cathodes in a Concentrated Lithium Salt Electrolyte," *Proc. 7th Int. Conf. Cold Fusion*, Vancouver, Canada, April 19–24, 1998, p. 43.

12. Y. ARATA and Y. C. ZHANG, "Achievement of Solid State Plasma Fusion (Cold Fusion)," *Proc. Int. Conf. Cold Fusion*, Toya, Japan, October 13–18, 1996, p. 129.

13. D. GOZZI, F. CELLUCCI, L. CIGNINI, G. GIGLI, M. TOMELLINI, E. CISBANI, S. FRULLANI, and G. M. URCIUOLI, "Erratum to X-Ray, Heath Excess and ^{4}He in the D/Pd System," *J. Electroanal. Chem.*, **435**, 251 (1997).

14. M. MILES and B. J. BUSH, "Search for Anomalous Effect Involving Excess Power and Helium During D_2O Electrolysis Using Palladium Cathodes," *Proc. 3rd Int. Conf Cold Fusion*, Nagoya, Japan, October 20–25, 1992, p. 189.

15. E. BOTTA, T. BRESSANI, D. CALVO, C. FANARA, and F. IAZZI, "Measurements of ^{4}He Production from D_2 Gas-Loaded Pd Sample," *Proc. 6th Int. Conf. Cold Fusion*, Toya, Japan, October 13–18, 1996, p. 29.

16. G. PREPARATA, "Some Theoretical Ideas," *Trans. Fusion Technol.*, **26**, 397 (1994).

17. H. HORA, J. C. KELLY, J. U. PATEL, M. A. PRELAS, G. H. MILEY, and J. W. TOMPKINS, "Screening in Cold Fusion Derived from D-D Reactions," *Phys. Lett. A*, **175**, 138 (1993).

18. P. L. HAGELSTEIN, "Anomalous Energy Transfer," *Proc. 7th Int. Conf. Cold Fusion*, Vancouver, Canada, April 19–24, 1998, p. 140.

19. M. R. SWARTZ, "Phusons in Nuclear Reactions in Solids," *Fusion Technol.*, **31**, 228 (1997).

20. V. VIOLANTE and A. DE NINNO, "Lattice Ion Trap: A Possible Mechanism Inducing a Strong Approach Between Two Deuterons in Condensed Matter," *Fusion Technol.*, **31**, 219 (1997).

21. V. VIOLANTE, A. TORRE, and G. DATTOLI, "Lattice Ion Trap: Classical and Quantum Description of a Possible Collision Mechanism for Deuterons in Metal Lattice," *Fusion Technol.*, **34**, *2*, 156 (1998).

22. V. VIOLANTE, "Lattice Ion-Trap Confinement for Deuterons and Protons: Possible Interaction in Condensed Matter," *Fusion Technol.*, **35**, 361 (1999).

23. J. M. ZIMAN, *Principles of the Theory of Solids*, 2nd ed., pp. 163–166, Cambridge University Press (1972).

24. C. KITTEL, *Quantum Theory of Solids*, p. 36, J. Wiley & Sons, New York, (1967).

25. A. M. BRODSKII, "Surface-Soliton Formation in Metal/Electrolyte Interface Electrodynamics," *Elektrokhim.*, **22**, *2*, 270 (1986).

26. A. M. BRODSKII and M. I. URBAKH, "Effect of Electrode Roughness on Photoemission During Surface-Plasmon Formation," *Elektrokhim.*, **17**, *3*, 302 (1981).

27. A. K. VIJH, "Electrode Potentials and Interface Plasmons in the Metal/Gaseous Electrolyte (i.e., Plasma) Interphasic Region," *Mater. Chem. Phys.*, **14**, 47 (1986).

28. V. M. AGRANOVICH and D. L. MILLS, *Surface Polaritons*, pp 331–403, North-Holland Publishing Company, Amsterdam (1982).

29. B. C. LAMARTINE, T. W. HAAS, and J. S. SOLOMON, *Appl. Surf. Sci.*, **4**, 537 (1980).

30. R. C. BROUWER and R. GRIESSEN, *Phys. Rev. Lett.*, **62**, 1760 (1989).

31. M. BALDO, R. PUCCI, and P. F. BORTIGNON, "Relaxation Toward Equilibrium in Plasmon-Enhanced Fusion," *Fusion Technol.*, **18**, 347 (1990).

32. M. GUPTA and J. P. BURGER, "The Electronic Structure and Its Relationship to Superconductivity in NiH, *J. Phys. F: Metal Phys.*, **10**, 2649 (1980).

33. G. PREPARATA, *QED Coherence in Matter*, p. 106, World Scientific (1995).

34. W. GREINER, *Quantum Mechanics*, p. 145, Springer-Verlag, New York (1989).

35. B. H. FLOWERS and F. MANDL, "Photodisintegration of the Alpha-Particle and the Inverse Process," *Proc. R. Soc. (London) A*, **206**, 131 (1951).

36. J. M. BLATT and V. F. WEISSKOPF, *Theoretical Nuclear Physics*, p. 344, John Wiley & Sons, New York (1960).

37. J. M. BLATT and V. F. WEISSKOPF, *Theoretical Nuclear Physics*, p. 420, John Wiley & Sons, New York (1960).

38. W. E. MEYERHOF, *Elements of Nuclear Physics*, p. 199, McGraw-Hill Book Company, New York (1989).

39. E. SEGRÈ, *Nuclei e Particelle*, 2nd ed., p. 433, Zanichelli (1962).

40. H. A. BETE and R. F. BACHER, *Rev. Modern Phys.*, **8**, 126 (1936).

41. M. FLEISCHMANN and S. PONS, "Electrochemically Induced Nuclear Fusion of Deuterium," *J. Electroanal. Chem.*, **261**, 301 (1989).

42. D. GOZZI et al., *Nuovo Cim. A*, **103**, 143 (1990).

43. E. STORM, "Review of Experimental Observations About the Cold Fusion Effect," *Fusion Technol.*, **20**, 433 (1991).

44. A. TAKAHASHI, M. KATSUHIKO, K. OCHIAI, and H. MIYAMARU, "Anomalous Enhancement of Three-Body Deuteron Fusion in Titanium-Deuteride with Low-Energy D^+ Beam Implantation," *Fusion Technol.*, **34**, 256 (1998).

45. J. KASAGI, H. YUKI, N. KASAJIMA, T. OHTSUKI, and A. G. LIPSON, "Anomalous Enhanced D(d,p)T Reactions in Pd and PdO Observed at Very Low Bombarding Energies," *Proc. 7th In. Conf. Cold Fusion*, Vancouver, Canada, April 19–24, 1998, p. 180.

46. C. ELSÄSSER, K. M. HO, C. T. CHAN, and M. FÄHNLE, "Vibrational States for Hydrogen in Palladium," *Phys. Rev. B*, **44**, *18*, 10377 (1991).

47. T. G. DOLAN, *Fusion Research, Vol. 1 Principles*, p. 30, Pergamon Press (1982).

48. S. R. CHUBB and T. A. CHUBB, *Fusion Technol.*, **24**, 403 (1993).

49. M. FLEISCHMANN, "More About Positive Feedback; More About Boiling," *Proc. 5th Int. Conf Cold Fusion*, Monte Carlo, Monaco, April 9–13, 1995, p. 140.

50. M. FLEISCHMANN and S. PONS, "Frontiers of Cold Fusion," *Proc. 3rd Int. Conf Cold Fusion*, Nagoya, Japan, October 21–25, 1992, p. 47

51. M. FLEISCHMANN and S. PONS, *Phys. Lett. A*, **176**, 118 (1993).

52. M. FLEISCHMANN, S. PONS, M. LE ROUX, and J. ROULETTE, *Proc. 4th Int. Conf. Cold Fusion*, Lahaina, Maui, Hawaii, December 6–9, 1993, Vol. 1, p. 1-1.

53. M. FLEISCHMANN, S. PONS, M. LE ROUX, and J. ROULETTE, *Trans. Fusion Technol.*, **26**, 323 (1994).

54. Y. IWAMURA, T. ITOH, N, GOTOH, M. SAKANO, and I. TOYODA, "Detection of Anomalous Elements, X-Ray and Excess Heat in a D_2-Pd System and Its Interpretation by the Electron-Induced Nuclear Reaction Model," *Fusion Technol.*, **33**, 476 (1998).

55. Y. KUCHEROV, "Slow Nuclear Excitation Model," *Proc. 6th Int. Conf. Cold Fusion*, Toya, Japan, October 13–18, 1996, Vol. 2, p. 502.

Vittorio Violante (chemical engineering degree, Naples University, Naples, Italy, 1979; PhD, new materials, Calabria University, Italy, 1992) is responsible for the Special Technology Section for Nuclear Fusion at ENEA Research Center of Frascati. He is involved in the ENEA research program for nuclear fusion; his field includes the interaction of hydrogen isotopes with materials, transport phenomena, tritium fuel cycle, and modeling.

Amalia Torre (PhD, physics, Naples University, Italy 1983) is senior scientist at ENEA Research Center of Frascati. Her main activities are in classical and quantum optics.

Giovanna Selvaggi [BS, physics, University of Rome, Italy; MS, nuclear engineering, University of Illinois at Urbana-Champaign (UIUC)] worked on the evaluation of the nuclear reaction probability for deuterons in condensed matter on the basis of a coherent behavior of the electron and deuteron plasmas in metal lattices. She collaborated in developing a software for a three-dimensional analysis of the lattice confinement effect on ion dynamics in condensed matter. She is currently working on her PhD in nuclear physics at UIUC on G0-Experiment to measure the parity-violating asymmetries in elastic electron-nucleon scattering.

George H. Miley (PhD, University of Michigan, 1958) is a professor in the Department of Nuclear Engineering and Electrical Engineering at UIUC. In addition, he is the founder and director of the Fusion Studies Laboratory at the University of Illinois. He is well known for his research on fusion, energy conversion, and nuclear-pumped lasers.